Elastic-plastic ductile damage model based on strain-rate plastic potential

Tudor Balan[1*] and Oana Cazacu[2]

[1]Laboratoire d'Etudes des Microstructures et de Mécanique des Matériaux, LEM3, UMR CNRS 7239, Arts et Métiers ParisTech, 4 rue A Fresnel, 57078 Metz Cedex 03, France.

[2] Department of Mechanical and Aerospace Engineering, University of Florida, REEF, 1350 N. Poquito Rd, Shalimar, FL 32579, USA.

ABSTRACT

Modeling of ductile damage is generally done using analytical potentials, which are expressed in the stress space. In this paper, for the first time it is shown that strain rate potentials which are exact conjugate of the stress-based potentials can be instead used to model the dilatational response of porous polycrystals. A new integration algorithm is also developed. It is to be noted that a strain-rate based formulation is most appropriate when the plastic flow of the matrix is described by a criterion that involves dependence on all stress invariants. In such cases, although a strain-rate potential is known, the stress-based potential cannot be obtained explicitly. While the proposed framework based on strain-rate potentials is general, for comparison purposes in this work we present an illustration of the approach for the case of a porous solid with von Mises matrix containing randomly distributed spherical cavities. Comparison between simulations using the strain-rate based approach and the classical stress-based Gurson's criterion in uniaxial tension is presented. These results show that the model based on a strain-rate potential predicts the dilatational response with the same level of accuracy.

Keywords: Porous solids; Strain rate potential; Spherical voids; Plasticity-damage couplings.

[*] Corresponding author: Tel: +33.387.375.460; fax: +33. .387.375.470
E-mail address: tudor.balan@ensam.eu

1. Introduction

Ziegler (1977) has shown that a plastic strain rate potential can be associated to any convex stress potential. Hence, a strain rate potential can be used instead of a classical stress potential to describe the plastic response of materials. Strain rate potentials are more suitable for process design, especially for solving inverse problems (e.g. Chung et al., 1997). Specifically, exact strain rate potentials associated to the von Mises, Hill (1948), or Cazacu et al. (2006) criteria have been used for metal forming simulations (e.g. Rabahallah et al., 2009a). Barlat and co-workers have also proposed several non-quadratic anisotropic strain rate potentials (for a review, see Kim et al., 2007). However, at present strain-rate potentials have been used only for the description of the plastic response of fully-dense metallic materials (void free materials). For such materials, yielding is insensitive to the mean stress and plastic deformation is not accompanied by any volume change. Therefore, the associated strain-rate potentials are expressed in terms of the deviator of the strain-rate tensor. As a consequence, all the existing time-integration algorithms based on strain-rate potentials make use of the hypothesis that the plastic flow is incompressible. However, most engineering materials contain defects (either cracks or voids). Early on it has been recognized that the presence of defects induces a dependence of the plastic response on the mean stress (Rice and Tracey, 1969; Tvergaard, 1981). To model the particularities of the plastic flow of voided polycrystals, micromechanically-motivated stress-based potentials have been developed. In particular, Gurson's (1977) is the most widely used criterion for modeling yielding of porous metals.

In this paper, it is shown that strain-rate potentials (SRP) can be instead used to numerically model damage-plasticity couplings. Illustration of this approach is done by considering the strain rate potential which is the exact conjugate of Gurson's (1977) stress-based potential for porous solids containing randomly distributed spherical voids. The structure of the paper is as follows. After a brief presentation of the kinematic homogenization approach of Hill-Mandel (Hill,1967; Mandel,1972), we recall Gurson's (1977) analysis and give the expression of the associated SRP (Section 2). The governing equations for an elastic-plastic damage model based on this SRP and the proposed time-integration algorithm are presented in Section 3. The developed algorithm is implemented in the FE code Abaqus/Standard as a user material subroutine (UMAT). For validation purposes, simulations of single-element uniaxial tension using the Abaqus built-in model and the developed UMAT are presented. Furthermore, in order to demonstrate the ability of the new SRP-based model to predict the salient features of ductile damage, an analysis of void volume fraction evolution in a notched tensile bar is conducted. Regarding notations, vector and tensors are denoted by boldface characters. If $\mathbf{A}$ and $\mathbf{B}$ are second-order tensors, the contracted tensor product between such tensors is defined as: $\mathbf{A}:\mathbf{B} = A_{ij}B_{ij}$ $i, j = 1\ldots3$. The norm of $\mathbf{A}$ is defined as $\|\mathbf{A}\| = \sqrt{\mathbf{A}:\mathbf{A}}$; tr denotes the trace of the tensor.

2. Modeling framework

Generally, the onset of plastic flow is described by specifying a convex yield function, $\varphi(\boldsymbol{\sigma})$, in the stress space and the associated flow rule

$$\mathbf{D}^{p} = \dot{\lambda}\frac{\partial \varphi}{\partial \boldsymbol{\sigma}}, \tag{1}$$

where $\boldsymbol{\sigma}$ is the Cauchy stress tensor, $\mathbf{D}^{\mathrm{p}}$ denotes the plastic strain rate tensor and $\dot{\lambda} \geq 0$ stands for the plastic multiplier. The yield surface is defined as $\varphi(\boldsymbol{\sigma}) = \tau$, where τ is a positive scalar with the dimension of stress. Generally, τ is taken as the uniaxial yield in tension, σ_{T}. The dual potential of the stress potential $\varphi(\boldsymbol{\sigma})$ is defined (see Ziegler (1977), Hill (1987)) as

$$\psi(\mathbf{D}^{\mathrm{p}}) = \dot{\lambda}, \tag{2}$$

and

$$\boldsymbol{\sigma} = \sigma_{\mathrm{T}} \frac{\partial \psi}{\partial \mathbf{D}^{\mathrm{p}}}. \tag{3}$$

The yield function $\varphi(\boldsymbol{\sigma})$ is generally taken homogeneous of degree one with respect to positive multipliers, so

$$\dot{\mathrm{W}}^{\mathrm{p}} = \sup_{\boldsymbol{\sigma} \in \mathbb{C}} \left(\sigma_{\mathrm{ij}} D_{\mathrm{ij}}^{\mathrm{p}} \right) = \dot{\lambda} \sigma_{\mathrm{T}}, \ \mathrm{i, j} = 1 \ldots 3, \tag{4}$$

where $\mathbb{C}$ is the convex domain delimited by the yield surface, and $\dot{\mathrm{W}}^{\mathrm{p}}$ is the work rate associated with the plastic strain rate tensor $\mathbf{D}^{\mathrm{p}}$. Thus, $\psi\left(\mathbf{D}^{\mathrm{p}}\right)$ is a work-equivalent measure of the strain rate. The functions $\psi\left(\mathbf{D}^{\mathrm{p}}\right)$ and $\varphi(\boldsymbol{\sigma})$ are dual potentials. For example, in the case of von Mises potential (i.e. $\varphi(\boldsymbol{\sigma}) = \sqrt{(3/2)\boldsymbol{\sigma}':\boldsymbol{\sigma}'}$), the associated SRP is: $\psi\left(\mathbf{D}^{\mathrm{p}}\right) = \sqrt{(2/3)\mathbf{D}^{\mathrm{p}}:\mathbf{D}^{\mathrm{p}}} = \dot{\bar{\varepsilon}}$, where $\dot{\bar{\varepsilon}}$ denotes the von Mises equivalent strain rate and $\boldsymbol{\sigma}'$ the stress deviator.

Plastic potentials for porous metallic materials

The kinematic homogenization approach of Hill-Mandel (Hill, 1967; Mandel, 1972) offers a rigorous framework for the development of criteria for describing the plastic response of porous solids. If the matrix is rigid-plastic, it has been shown (e.g. Talbot and Willis, 1985) that there exists a strain-rate potential $\Pi = \Pi(\mathbf{D}^{p}, f)$ such that the stress at any point in the porous solid is given by:

$$\boldsymbol{\sigma} = \frac{\partial \Pi\left(\mathbf{D}^{\mathrm{p}}, f\right)}{\partial \mathbf{D}^{\mathrm{p}}} \text{ with } \Pi\left(\mathbf{D}^{\mathrm{p}}, f\right) = \inf_{\mathbf{d} \in K(\mathbf{D})} \left\langle \pi(\mathbf{d}) \right\rangle_{\Omega}. \tag{5}$$

where Ω is a representative volume element composed of the matrix and a traction-free void, while $\langle\ \rangle$ denotes the average value over Ω; f is the porosity (ratio between the volume of the void and the volume of Ω); $\pi(\mathbf{d})$ is the matrix's plastic dissipation with $\mathbf{d}$ being the local plastic strain rate tensor. Minimization is done over $K(\mathbf{D})$, which is the set of incompressible velocity fields compatible with homogeneous strain-rate boundary conditions, i.e.

$$\mathbf{v} = \mathbf{D}\,\mathbf{x}, \text{ for any } \mathbf{x} \in \partial\Omega. \tag{6}$$

Only very few velocity fields compatible with uniform strain-rate boundary conditions are known. For example, for spherical void geometry the only known velocity fields are those deduced by Rice and Tracey (1969) and Budiansky et al. (1982). For examples of other

velocity fields deduced using an Eshelby-type approach, the reader is referred to Monchiet et al. (2011). Furthermore, in order to arrive at closed-form expressions, the local plastic dissipation is calculated for a unique velocity field. Thus, the associated overall potential is an upper-bound of the exact plastic dissipation of the porous solid. However, only in the case when the plastic behavior of the matrix is described by simple expressions (e.g. von Mises, Hill, 1948), it is possible to arrive at a closed-form expression of the approximate stress-based plastic potentials of the porous solid (e.g. Gurson, 1977; Monchiet et al. 2008, respectively). If the plastic flow of the matrix is described by a criterion involving all stress invariants, e.g. Tresca criterion, an approximate SRP can be deduced (see Appendix A); however, a closed-form stress-based criterion can be obtained only in parametric form (see Cazacu et al., 2013). Furthermore, integration algorithms exist only for stress-based formulations of coupled elasto-plastic damage behavior (e.g. Aravas, 1987). Although all the numerical methods and techniques developed in this paper are valid for an elasto-plastic damage model described by a general strain-rate potential $\Pi = \Pi(\mathbf{D}^p, f)$ in its general form, in this paper we discuss a specific strain-rate potential which is the exact conjugate of Gurson's (1977) stress potential for spherical cavities. Let us recall that the analysis of Gurson (1977) was done on a hollow-sphere, its rigid-plastic behavior being governed by the von Mises yield criterion. The local plastic dissipation was calculated using the velocity field deduced by Rice and Tracey (1969). The approximate strain-rate potential obtained is:

$$\Psi\left(\mathbf{D}^p, f\right) = 2\left|D_m^p\right|\left[\frac{\sqrt{1+u^2}-\sqrt{f^2+u^2}}{u}+\ln\left(\frac{u+\sqrt{f^2+u^2}}{u+\sqrt{1+u^2}}\frac{1}{f}\right)\right]. \tag{7}$$

where f denotes the porosity (or void volume fraction), $u = 2\left(\left|D_m^p\right| / D_e^p\right)$, with $D_m^p = \left(tr\,\mathbf{D}^p\right)/3$ and $D_e^p = \sqrt{(2/3)\mathbf{D}'^p : \mathbf{D}'^p}$. Hence, at yielding:

$$\frac{\sigma_m}{\sigma_T} = \frac{1}{3}\frac{\partial\Psi\left(\mathbf{D}^p, f\right)}{\partial D_m^p} = \frac{2}{3}\ln\left(\frac{u+\sqrt{u^2+f^2}}{u+\sqrt{u^2+1}}\cdot\frac{1}{f}\right), \tag{8a}$$

$$\frac{\sigma_e}{\sigma_T} = \left|\frac{\partial\Psi\left(\mathbf{D}^p, f\right)}{\partial D_e^p}\right| = \sqrt{1+u^2}-\sqrt{u^2+f^2}\,. \tag{8b}$$

where $\sigma_m = tr(\boldsymbol{\sigma})/3$ and $\sigma_e = \sqrt{(3/2)\boldsymbol{\sigma}' : \boldsymbol{\sigma}'}$. The parameter u can be eliminated between Eqs. (8), to arrive at the classical stress-based formulation (for details, see Gurson, 1977):

$$\Phi(\boldsymbol{\sigma}, f) = \left(\frac{\sigma_e}{\sigma_T}\right)^2 + 2f\cosh\left(\frac{3\sigma_m}{2\sigma_T}\right) - 1 - f^2. \tag{9}$$

As an example, in Figure 1(a) is shown the representation of the strain-rate potential (7) for different initial porosities $f = 0.001$, $f = 0.01$, and $f = 0.1$, respectively, while in Figure 1(b) are shown isocontours of its exact dual, i.e. Gurson's stress potential (Eq. (9)) for the same porosities. The porous material being isotropic, the principal directions of $\mathbf{D}^p$ and stress coincide. The projection of the strain-rate potential in the octahedral plane (plane with normal at equal angles to the principal directions of the strain rate tensor $\mathbf{D}^p$) is shown in Figure 2(a) while Figure 2(b) depicts the section of Gurson's (1977) stress potential.

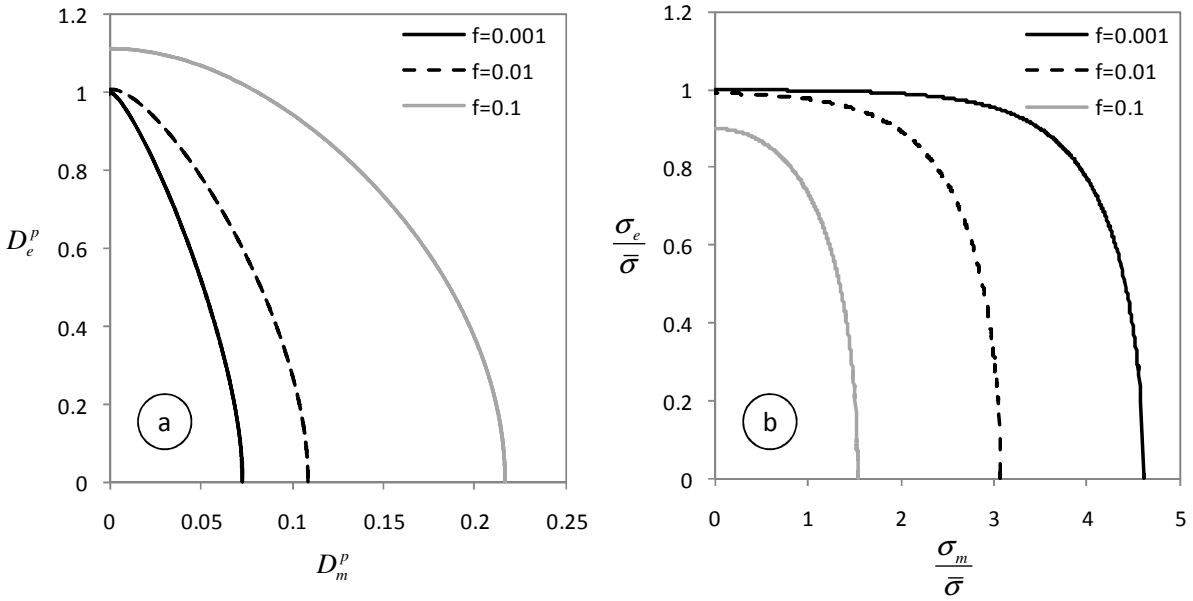

Figure 1. Strain-rate potential (a) and normalized yield surface (b) for fixed values of the porosity *f*.

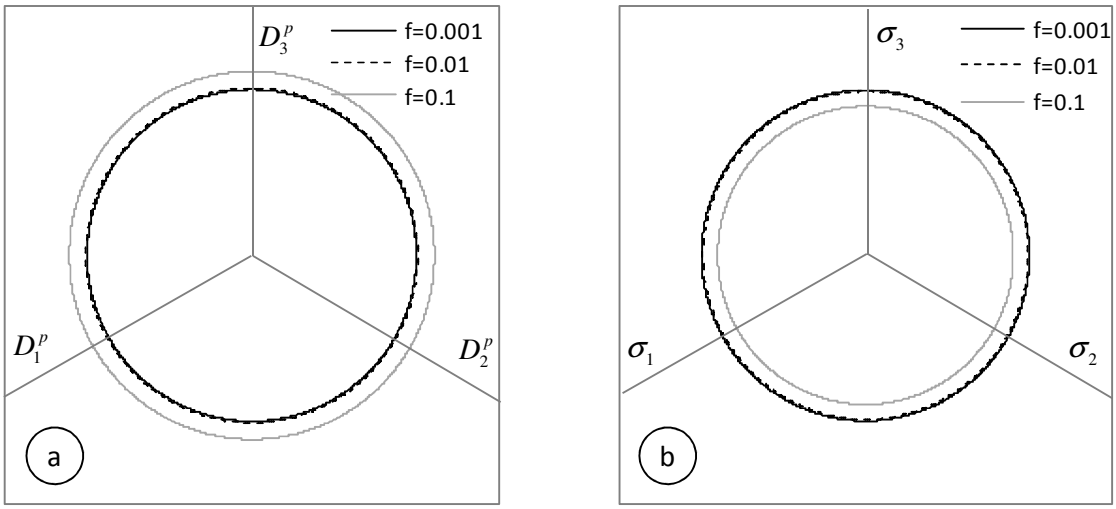

Figure 2. (a) Section of the SRP with $D_m^p = 0$; (b) octahedral plane representation of its dual, Gurson's normalized yield surface potential for $\sigma_m = 0$ for fixed values of the porosity *f*.

3. Time-integration algorithm for a general elastic-plastic damage model based on a strain-rate plastic potential

In the following we present the governing equations for an elastic-plastic damage model based on a strain rate potential and a general time-integration algorithm. The total rate of deformation is considered to be the sum of an elastic part and a plastic part $\mathbf{D}^p$. The elastic

response is described by Hooke's law. In the plastic regime, stresses are derived from a strain-rate potential, i.e.:

$$\boldsymbol{\sigma} = \bar{\sigma}\frac{\partial \Psi}{\partial \mathbf{D}^p}, \tag{10}$$

In Eq.(10), $\bar{\sigma}$ is the tensile effective stress for the matrix (fully-dense material), whose hardening is considered to be governed by the local effective plastic strain, $\bar{\varepsilon}$ according to a power law of the form:

$$\bar{\sigma} = A\left(\varepsilon_0 + \bar{\varepsilon}\right)^n. \tag{11}$$

The rate of the local effective plastic strain $\dot{\bar{\varepsilon}}$ is obtained, assuming the equivalence of microscopic and macroscopic plastic work as

$$\bar{\sigma}\dot{\bar{\varepsilon}}\left(1-f\right) = \boldsymbol{\sigma} : \mathbf{D}^p. \tag{12}$$

The porosity evolution law is supposed of the generic form

$$\dot{f} = \dot{f}\left(\mathbf{D}^p, \bar{\varepsilon}, \dot{\bar{\varepsilon}}\right). \tag{13}$$

Loading-unloading condition

In classical rate-independent plasticity, the yield function is used in order to determine whether a given stress state corresponds to elastic or elasto-plastic loading. In the case of an SRP-based formulation, no explicit yield condition is available, so alternative loading/unloading conditions need to be considered (e.g. Van Houtte et al., 1995). Let define

$$g\left(\mathbf{N}\right) = \Psi\left(\mathbf{N}\right) - \frac{\boldsymbol{\sigma}}{\bar{\sigma}} : \mathbf{N}, \tag{14}$$

where $\mathbf{N}= \mathbf{D}^p / \left\|\mathbf{D}^p\right\|$ is the normalized plastic strain rate tensor. The loading/unloading condition proposed by Bacroix and Gilormini (1995) will be adopted. It is based on the maximum work principle

$$\underset{\mathbf{N}}{\text{Min}}\, g\left(\mathbf{N}\right) \begin{cases} < 0 & \text{if } \boldsymbol{\sigma} \text{ is outside the yield surface,} \\ = 0 & \text{if } \boldsymbol{\sigma} \text{ is on the yield surface,} \\ > 0 & \text{if } \boldsymbol{\sigma} \text{ is inside the yield surface.} \end{cases} \tag{15}$$

It is to be noted that in classical elastic/plastic formulations, $\mathbf{D}^p$ is symmetric and deviatoric, so the minimization is done with respect to the four independent components of the normalized tensor (see Rabahallah et al., 2009b). In the case of a coupled plasticity-damage model, $\mathbf{D}^p$ is no longer deviatoric, the SRP also depending on tr ($\mathbf{D}^p$) (for example, see Eq. (7)). It is proposed to use five independent angles, to define the five independent components of the unit-length tensor **N**:

$$
\begin{aligned}
N_1 = N_{11} &= \sin\theta_1 \sin\theta_2 \sin\theta_3 \sin\theta_4 \sin\theta_5 \\
N_2 = N_{22} &= \cos\theta_1 \sin\theta_2 \sin\theta_3 \sin\theta_4 \sin\theta_5 \\
N_3 = N_{33} &= \cos\theta_2 \sin\theta_3 \sin\theta_4 \sin\theta_5 \\
N_4 = \sqrt{2}N_{12} &= \cos\theta_3 \sin\theta_4 \sin\theta_5 \\
N_5 = \sqrt{2}N_{23} &= \cos\theta_4 \sin\theta_5 \\
N_6 = \sqrt{2}N_{31} &= \cos\theta_5
\end{aligned}
, \qquad (16)
$$

where $0 \le \theta_1 \le 2\pi$ and $0 \le \theta_i \le \pi$, for $i = 2 \ldots 5$; and let denote $\boldsymbol{\theta} = (\theta_1, \theta_2, \theta_3, \theta_4, \theta_5)$. The minimization of g with respect to $\boldsymbol{\theta}$ is associated with the solution of the equation $\partial g(\boldsymbol{\theta}) / \partial \boldsymbol{\theta} = 0$. Let us note that this minimization can be avoided in several cases. During plastic loading, when the initial stress $\boldsymbol{\sigma}_n$ already lies on the yield surface, the following condition $(\boldsymbol{\sigma}^{try} - \boldsymbol{\sigma}_n) : \mathbf{N}_n \ge 0$ guarantees that the trial stress is outside the yield surface (Hughes, 1984), where $\mathbf{N}_n$ is the normal to the initial yield surface, which can be stored at each increment for future use. This condition renders the minimization unnecessary in most situations. However, when the minimization is required, it can be stopped as soon as a tensor $\mathbf{N}$ is found so that $g(\mathbf{N})<0$. Indeed, the minimum is guaranteed to be negative in this case, so the increment is elasto-plastic. In practice, several simple initializations for $\mathbf{N}$ already fulfil this condition in most cases. Thus, the minimization procedure seldom needs more than one iteration, the computational cost being equivalent to that for stress-based plasticity-damage formulation (e.g. Eq. (9)).

4. Examples: Analysis of void volume fraction evolution in uniaxial tension

At present, solution of boundary-value problems in ductile damage are done using finite-element methods and the stress-based potential $\Phi(\boldsymbol{\sigma}, f)$ given by Eq. (9). One of the objectives of this paper is to show that one can use instead an SRP formulation and function $\Psi(\mathbf{D}^p, f)$ given by Eq. (7), which is the exact conjugate of $\Phi(\boldsymbol{\sigma}, f)$. The general time-integration algorithm developed was applied to $\Psi(\mathbf{D}^p, f)$ given by Eq. (7) and implemented in the FE code Abaqus Standard. To illustrate the capabilities of the new formulation, FE analyses of void volume fraction evolution during tensile tests are performed. For both formulations (SRP based, and stress-potential based), the material parameters include the elastic properties of the matrix: $E/\sigma_T = 300$, $\nu = 0.3$, where E is the Young modulus and ν is the Poisson coefficient, and the parameters involved in the matrix's hardening law ($A/\sigma_T = 1.8$; $\varepsilon_0 = 0.003$; $n = 0.1$). The initial void volume fraction considered in all simulations is $f_0 = 0.00014$. Void nucleation is described by the classical law of Chu and Needleman (1980); the generic porosity evolution, given by Eq. (13), thus becomes:

$$
\dot{f} = \frac{f_N}{s_N\sqrt{2\pi}} \exp\left[-\frac{1}{2}\left(\frac{\bar{\varepsilon} - \varepsilon_N}{s_N} \right)^2 \right] + (1-f)\,\mathbf{D}^p : \mathbf{I}\,, \qquad (17)
$$

where the values of the nucleation parameters are $f_N = 0.04$; $s_N = 0.1$ and $\varepsilon_N = 0.3$. The numerical values for all material parameters are taken from Tvergaard and Needleman (1984)

and Aravas (1987). This allows for partial verification of the FE implementation based on strain-rate plastic potential through comparison with the results obtained with the ABAQUS built-in Gurson model that uses the classical stress-based approach, with the potential given by Eq. (9). First, a uniform tensile loading of a single finite element is performed using the developed SRP-based material routine and the Abaqus built-in model. The evolutions of the tensile stress and porosity as predicted by both approaches are compared in Fig. 3. Clearly, the same results are obtained.

For a more realistic simulation of a tensile test, a round tensile bar geometry is also considered. The FE mesh consists of 2325 hexahedral linear elements with reduced integration (Abaqus C3D8R element, Abaqus, 2009) (see also Fig.4). Displacement boundary conditions are applied at the end of the specimen until the maximum porosity in the bar reaches the value $f = 0.062$. Comparison between the load-displacement responses according to the two formulations is shown in Figure 5. It is clearly seen that the results obtained with the ABAQUS built-in model and algorithm and with our UMAT implementation are identical. Fig. 6 shows isocontours of the void volume fraction corresponding to the end of each test.

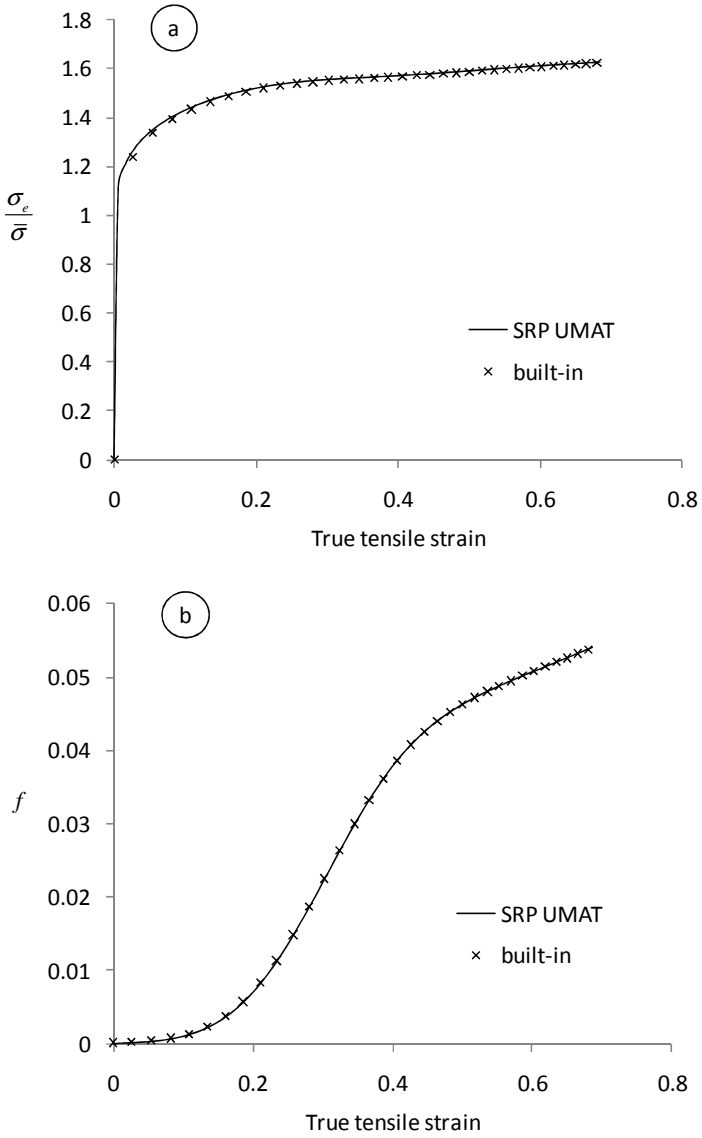

Figure 3. Evolutions of (a) tensile stress and (b) porosity in uniaxial tension as obtained with the developed UMAT for the SRP-potential given by Eq.(7) using the developed algorithm, in comparison with the Abaqus built-in model that uses Gurson's stress potential (Eq. (9)) and Aravas (1987) algorithm. Simulations are done using a single-element (ABAQUS C3D8R element).

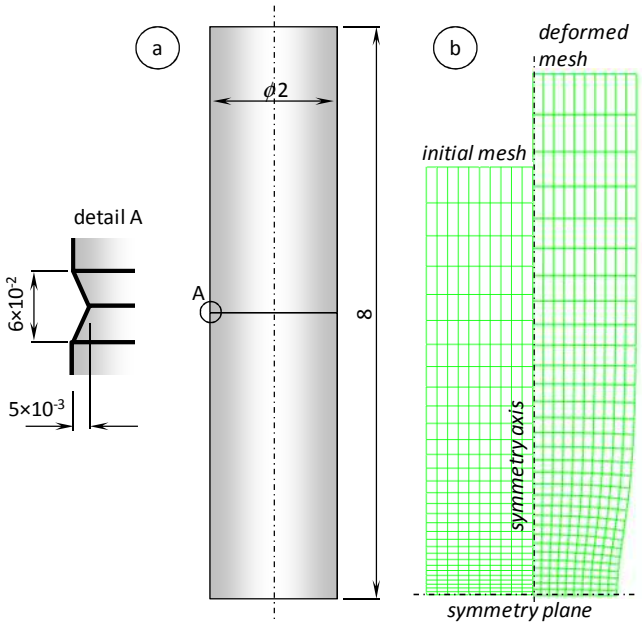

Figure 4. (a) Geometry of the sample and imperfection; (b) FE mesh of one eight of the sample.

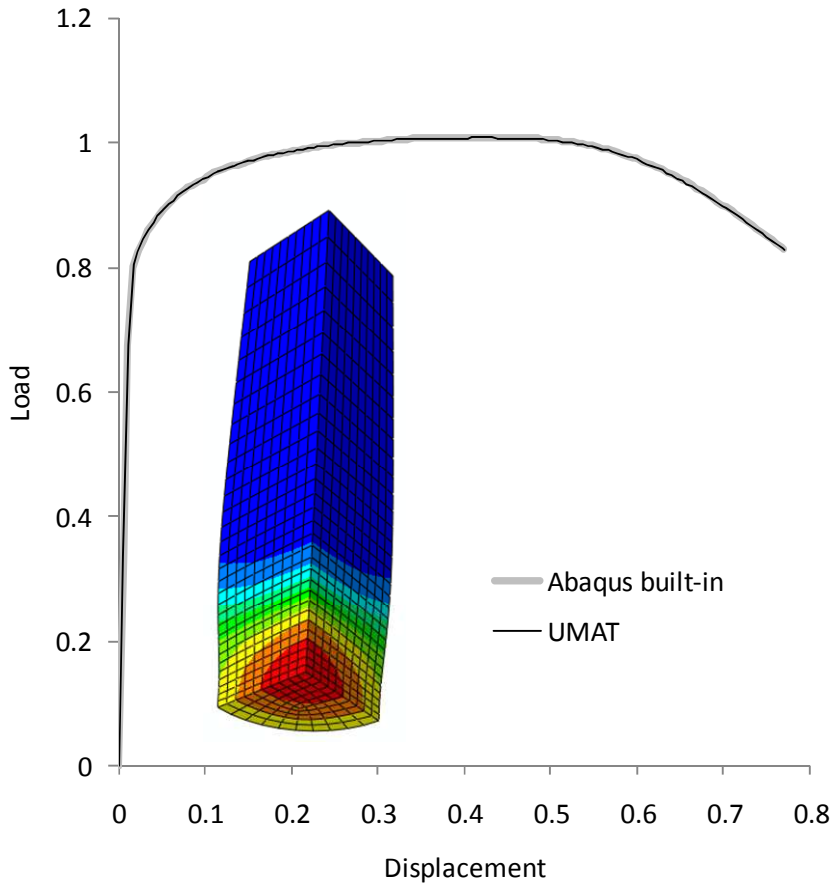

Figure 5. Load-displacement curve predicted with the proposed approach and with the ABAQUS built-in model, respectively.

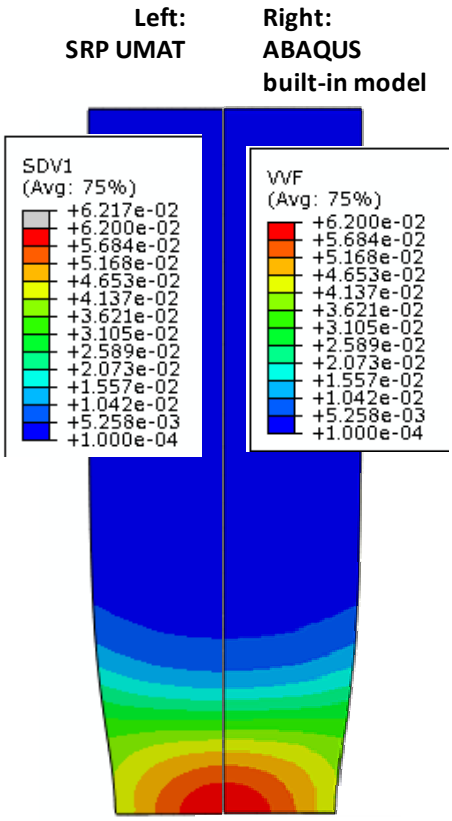

Figure 6. Isocontours of the void volume fraction at the end of each test, as predicted using (left) the strain-rate based formulation and algorithm developed in this paper, and (right) the ABAQUS built-in model that uses Gurson's potential (Eq. (9)).

4. Conclusions and Perspectives

It was shown that a strain rate potential that is the exact dual of the stress-based potential of Gurson (1977) for spherical voids can be used to describe the response of porous materials. Based on the presented results, it is believed that a very good description of the plastic behavior for large strains can be obtained by using strain rate potentials. Such formulations are particularly suitable for design optimization. In this paper illustration of the approach was presented for the dual of Gurson's (1977) stress-based potential for porous solids containing randomly distributed spherical voids. However, the framework and time-integration algorithm is general and can be applied to the description of ductile damage irrespective of the plastic response of the matrix. Such a strain-rate based approach is most appropriate for porous materials with matrix described by complex yield criteria for which a closed-form expression of the stress-based potential cannot be obtained explicitly.

References

Abaqus. User's Manual for Version 6.8. Volumes I–V. Dassault Systemes Simulia Corp., Providence, RI., 2009.

Aravas, N., 1987. On the numerical integration of a class of pressure-dependent plasticity models, Int. J. Num. Meth. Eng. 24, 1395–1416.

Bacroix, B., Gilormini, P., 1995. Finite-element simulations of earing in polycrystalline materials using a texture-adjusted strain-rate potential, Model. Mater. Sci. Eng. 3, 1–21.

Budyanski, B., Hutchinson, J., Slutsky, S., 1982. Void growth and collapse in viscous solids. In: Hopkins, H.G. and Sewell, M.J. (ed.), Mechanics of Solids, The Rodney Hill 60th Anniversary Volume, Pergamon Press, Oxford, 13-45.

Cazacu, O., Plunkett, B., Barlat, F., 2006. Orthotropic yield criterion for hexagonal closed packed metals. Int. J. Plasticity 22, 1171-1194.

Cazacu, O., Revil-Baudard, B., Chandola, N., Kondo, D. 2013. New analytic criterion for porous solids with Tresca matrix for axisymmetric loadings. Int. J. Solids. Structures (accepted).

Chu, C.C., Needleman, A., 1980. Void nucleation effects in biaxially stretched sheets. J. Engng. Mater. Technol. – Trans ASME 102, 249-256.

Chung, K., Barlat, F., Brem, J.C., Lege, D.J., Richmond, O., 1997. Blank shape design for a planar anisotropic sheet based on ideal forming design theory and FEM analysis, Int. J. Mech. Sciences 39, 105–120.

Gurson, A. L., 1977. Continuum theory of ductile rupture by void nucleation and growth: Part I : Yield criteria and flow rules for porous ductile media. J. Engng. Matl. Tech. Trans. ASME, Series H, 99, 2-15.

Hill, R., 1948. A theory of yielding and plastic flow of anisotropic metals. Proc. Roy. Soc. London A 193, 281-297.

Hill, R., 1967. The essential structure of constitutive laws for metal composites and polycrystals. Journal of the Mechanics and Physics of Solids 15, 79–95.

Hill, R., 1987. Constitutive dual potentials in classical plasticity. J. Mech. Phys. Solids 35, 23-33.

Hughes, T.J.R., 1984. Numerical implementation of constitutive models: rate-independent deviatoric plasticity, In Theoretical Foundation for Large-scale Computations for Nonlinear Material Behavior, Nemat-Nasser, S., Asaro, R.J., Hegemier, G.A. (eds), Martinus Nij Publishers: Dordrecht, The Netherlands, 29–57.

Kim, D., Barlat, F., Bouvier, S., Raballah, M., Balan, T., Chung, K., 2007. Non-quadratic anisotropic potentials based on linear transformation of plastic strain rate. Int. J. of Plasticity 23, 1380-1399.

Mandel, J., 1972. Plasticite classique et viscoplasticite, Int. Centre Mech Sci., Courses and lectures, 97, Udine 1971, Springer, Wien, New York.

Monchiet, V., Cazacu, O., Charkaluk, E. and Kondo, D., 2008. Macroscopic yield criteria for plastic anisotropic materials containing spheroidal voids. Int. J. Plasticity, 24, 1158-1189.

Monchiet, V., Charkaluk, E., and Kondo, D., 2011, A micromechanics-based modification of the Gurson criterion by using Eshelby-like velocity fields, European Journal of Mechanics - A/Solids 30, 940-949.

Rabahallah, M., Balan, T., Bouvier, S., Bacroix, B., Barlat, F., Chung, K., Teodosiu, C., 2009a. Parameter identification of advanced plastic potentials and impact on plastic anisotropy prediction, Int. J. Plasticity 25, 491–512.

Rabahallah, M., Balan, T., Bouvier, S., Teodosiu, C., 2009b. Time integration scheme for the finite element implementation of elasto-plastic models based on anisotropic strain-rate potentials, Int. J. Num. Meth. Eng. 80, 381–402.

Rice, J.R., Tracey, D.M., 1969. On the ductile enlargement of voids in triaxial stress fields. J. Mech. Phys. Solids 17, 201–217.

Talbot, D. R. S. and Willis, J. R., 1985. Variational principles for inhomogeneous non-linear media, IMA J Applied Mathematics, 35(1), 39-54.

Tvergaard, V., 1981. Influence of voids on shear band instabilities under plane strain conditions. Int. J. Fracture 17 (4), 389–407.

Tvergaard, V., Needleman, A., 1984. Analysis of the cup-cone fracture in a round tensile bar. Acta Met. Mater. 32, 157–169

Van Houtte, P., Van Bael, A., Winters, J., 1995. The incorporation of texture-based yield loci into elasto-plastic finite element programs, Textures and Microstructures 24, 255–272.

Ziegler, H., 1977. An introduction to thermodynamics, North-Holland, Amsterdam.

Appendix A: SRP of a porous solid with Tresca matrix for axisymmetric strain paths

For axisymmetric conditions, the plastic strain rate can be written in the form: $\mathbf{D}^p = \mathrm{D}_{11}^p\left(\mathbf{e}_1\otimes\mathbf{e}_1+\mathbf{e}_2\otimes\mathbf{e}_2\right)+\mathrm{D}_{33}^p\left(\mathbf{e}_3\otimes\mathbf{e}_3\right)$, with ($\mathbf{e}_1$, $\mathbf{e}_2$, $\mathbf{e}_3$) being the unit vectors of a Cartesian coordinate system. The SRP corresponding to a porous solid described by the Tresca criterion and containing spherical voids is an even function in $\mathbf{D}^p$ (Cazacu et al.,2013). Thus, only the expression of the SRP for the cases when ($D_m^p \geq 0$ and $D_{11}'^p \geq 0$) and ($D_m^p \geq 0$ and $D_{11}'^p \leq 0$) is given in the following; for all other axisymmetric strain paths the expression is obtained by symmetry.

(i) For $D_m^p \geq 0$ and $D_{11}'^p \geq 0$:

$$\begin{cases} \Psi\left(\mathbf{D}^p\right)=\dfrac{D_m^p}{8}\left(F_1\left(u/f\right)-F_1\left(u\right)\right) \quad ,\forall\ u<f \\ \Psi\left(\mathbf{D}^p\right)=\dfrac{D_m^p}{8}\left(F_2\left(u/f\right)-F_1\left(u\right)\right),\forall\ f<u<1 \\ \Psi\left(\mathbf{D}^p\right)=\dfrac{D_m^p}{8}\left(F_2\left(u/f\right)-F_2\left(u\right)\right),\forall\ u>1 \end{cases} \tag{A.1}$$

with

$$\begin{aligned} F_1(y)&=1-16\ln(2)-\frac{6}{y}+\frac{\left(3y^2+8y^{3/2}+6y-1\right)}{y^{3/2}}\ln\left(\frac{\sqrt{y}+1}{1-\sqrt{y}}\right)+16\ln\left(1-\sqrt{y}\right) \\ F_2(y)&=1-16\ln(2)-\frac{6}{y}+\frac{\left(3y^2+8y^{3/2}+6y-1\right)}{y^{3/2}}\ln\left(\frac{\sqrt{y}+1}{\sqrt{y}-1}\right)+16\ln\left(\sqrt{y}-1\right) \end{aligned} \tag{A.2}$$

(ii) For $D_m^p \geq 0$ and $D_{11}'^p \leq 0$:

$$\begin{cases} \Psi\left(\mathbf{D}^p\right) = \dfrac{D_m^p}{8}\left(G_1\left(u/f\right) - G_1\left(u\right)\right) & ,\forall\ u < f \\ \Psi\left(\mathbf{D}^p\right) = \dfrac{D_m^p}{8}\left(G_2\left(u/f\right) - G_1\left(u\right) - 12 - 16\ln\left(2\right)\right), & \forall\ f < u < 1 \\ \Psi\left(\mathbf{D}^p\right) = \dfrac{D_m^p}{8}\left(G_2\left(u/f\right) - G_2\left(u\right)\right), & \forall\ u > 1 \end{cases} \qquad \text{(A.3)}$$

with:

$$\begin{aligned} G_1(y) &= -\frac{6}{y} - \arctan\left(\frac{2\sqrt{y}}{y-1}\right)\frac{\left(3y^2 - 6y - 1\right)}{y^{3/2}} - 8\ln\left(y+1\right) \\ G_2(y) &= \frac{6}{y} + \frac{\left(3y^2 - 6y - 1\right)}{y^{3/2}}\arcsin\left(\frac{2\sqrt{y}}{y+1}\right) + 8\ln\left(y+1\right) \end{aligned} \qquad \text{(A.4)}$$